Analysis of intensity effects in laser electron-beam backscattering in terms of generalised Bessel functions

1981 J. Phys. A: Math. Gen. 14 509

(http://iopscience.iop.org/0305-4470/14/2/026)

J. Phys. A: Math. Gen. **14** (1981) 509–520. Printed in Great Britain

Analysis of intensity effects in laser electron-beam backscattering in terms of generalised Bessel functions

C Leubner† and Eva M Strohmaier

Theoretical Physics Institute, University of Innsbruck, A-6020 Innsbruck, Austria

Received 25 June 1980, in final form 11 August 1980

Abstract. Within the framework of classical electrodynamics, we present a quantitative analysis of the intensity-dependent distribution in frequency and angle of the spontaneous incoherent radiation that arises from the collision of a beam of relativistic electrons with a very intense, linearly polarised plane electromagnetic wave. As a useful corollary, this investigation establishes a uniform asymptotic expansion of an important class of functions that frequently occurs in the literature under the name of 'generalised Bessel functions', but for which to date only qualitative results are employed for the most interesting range of large values of its variables.

1. Introduction

Stimulated by the successful observation of frequency up-conversion and power gain in microwave scattering from a relativistic electron beam front (Granatstein *et al* 1976, Buzzi *et al* 1977, Pasour *et al* 1977), as first predicted by Motz (1951) and Landecker (1952), and by the current availability of very high-power electromagnetic radiation in the near-infrared through the glass laser technology, we have reconsidered the classical problem of Goldman (1964) who studied the intensity-dependent modifications to Klein–Nishina's formula in the spontaneous inverse Compton scattering arising from the reflection of a high-intensity laser pulse from relativistic electrons.

This reconsideration was motivated by the fact that although Goldman (1964) gave the integral representation of the pertinent differential cross section for the general case of an elliptically polarised incident laser beam, he was only able to reduce this cross section to closed form for the particular case of circular polarisation, where it can be expressed through a finite number of ordinary Bessel functions of integer order. However, circular polarisation of the incident beam is of little relevance, since the nonlinear effects under study, in order to dominate the emitted radiation pattern, require the most powerful laser systems currently available, which as is well known have to be constructed for practical reasons so as to emit linearly polarised light, which—again for practical reasons—cannot be converted to circularly polarised light. Hence, the only case of experimental interest is the evaluation of Goldman's cross section for linear incident polarisation.

This fact alone would perhaps not justify devoting a separate investigation to Goldman's problem for linear incident polarisation, in particular, as the cross section

†Present address: Max-Planck-Institut für extraterrestrische Physik, D-8046 Garching, Germany.

0305-4470/81/020509+12$01.50

presented in § 2 derives from a considerably simplified model of the real situation on the one hand, and on the other places extreme requirements on the intensity of the primary light source, although a number of theoretical investigations have recently been based on the availability of laser intensities of 10^{18} W cm^{-2} and more in the near future (see e.g. Waltz and Manley 1978, Tajima and Dawson 1979). But the point is that for linear incident polarisation Goldman's cross section is expressible through a finite number of so-called 'generalised Bessel functions', an important class of functions, which frequently occurs in the literature in the study of various elementary scattering processes in the simultaneous presence of an intense, linearly polarised laser field, for which a description in the electric dipole approximation is inadequate (see e.g. Brown and Kibble 1964, Yakovlev 1966, Oleinik 1967, Denisov and Fedorov 1968, Brehme 1971, Lyul'ka 1975, 1977, Ehlotzky 1978, Kelsey and Rosenberg 1979, Schlessinger and Wright 1979). While, in the uninteresting case of such small intensities that the process under study differs very little from the corresponding one without the presence of a laser field, the generalised Bessel functions can be expanded in a rapidly convergent series of products of ordinary Bessel functions (Brown and Kibble 1964, Ehlotzky 1978, Kelsey and Rosenberg 1979), this procedure is not feasible in the interesting case of high intensities, and in fact none of the above references indicates an efficient method to evaluate these functions under these circumstances. Such a method is urgently called for, however, in order to assess the magnitude of some of the effects involved in more than just a rough qualitative manner and in order to compare quantitatively the results of different approaches.

We will therefore take the following evaluation of Goldman's cross section for a linearly polarised incident laser beam as an occasion to discuss in detail and in a self-contained way the derivation of an asymptotic expansion of the generalised Bessel functions, which is uniformly valid for such intensities where the standard methods are inapplicable.

2. Model and differential scattering cross section

As a model for the spontaneous incoherent scattering arising from the collision of a relativistic electron beam with an intense laser pulse, we consider the following simplified process, which was originally studied by Goldman (1964). A homogeneous beam of relativistic electrons is travelling with uniform velocity along the negative z-axis of some Cartesian coordinate system. This model beam differs from a realistic situation by the neglect of both a density gradient and a velocity distribution. In our model we furthermore assume the density to be low enough so that collective effects among the electrons can be neglected. This electron beam is taken to collide with a very intense pulse of near-infrared laser radiation, propagating along the positive z-axis and being linearly polarised in the x direction, which is described by a plane wave, neglecting the fact that in an experiment an extremely powerful laser system would have to be very tightly focussed in order to reach the threshold of 10^{18} W cm^{-2} (Tajima and Dawson 1979), beyond which the scattered radiation is dominated by the nonlinearities of the interaction. If, as a final simplifying assumption, radiation reaction is neglected, then the pertinent cross section for the distribution of the scattered radiation in frequency and angle is standard and has been used by a number of authors.

In order to save space, we rely on results and notation of related work (Leubner 1978), where the single-particle cross section, corresponding to the appropriate regime

of incoherent scattering (because of the envisaged optical primary wavelength (Stolyarov 1977)), was found from a purely classical investigation to be given by

$$\frac{\mathrm{d}\sigma(\omega)}{\mathrm{d}\Omega} = \sum_{l=1}^{\infty} \delta\left(\omega - \frac{l\omega_i}{w}\right)\left(\frac{r_0 l}{\pi\mu w^2}\right)^2 |\boldsymbol{s}\times\boldsymbol{I}_l|^2, \tag{1}$$

where

$$\boldsymbol{I}_l = -\int_0^{2\pi}\left[\boldsymbol{e}_x\left(\mu\cos\frac{\eta}{b}\right) + \boldsymbol{e}_z\left(1+\cos\phi\sin\vartheta\mu\cos\frac{\eta}{b}\right)\Big/(1-\cos\vartheta)\right]\exp[lF(\eta)]\,\mathrm{d}\eta \tag{2}$$

(where a partial integration on the z component of $\boldsymbol{I}_l$ has been performed in order to restrict the parameter λ in (5) to only two values $\lambda = 0, 1$) and

$$F(\eta) = \mathrm{i}\{\eta + [2v\nu\sin\eta + (\nu^2/4)\sin 2\eta]/w\}. \tag{3}$$

$\mathrm{d}\sigma(\omega)/\mathrm{d}\Omega$ is the scattered power per unit incident intensity, per unit band width and per unit solid angle, and the meaning of the other symbols in (1)–(3) is as follows. $r_0 = e^2/mc^2$ is the classical electron radius, $b = [(1+\beta_0)/(1-\beta_0)]^{1/2}$, with the initial velocity $\boldsymbol{\beta}_0 = -\beta_0\boldsymbol{e}_z$ of the electron. $\omega = \omega_i(t - z/c)$ is the phase of the incoming electromagnetic wave, with ω_i being the incident frequency as measured in the laboratory frame, in which we work throughout, and $\mu = eE_0/mc\omega_i$ is the intensity parameter with E_0 the electric field strength of the incoming wave. $\boldsymbol{s}$ is the direction of observation with components $(\cos\phi\sin\vartheta, \sin\phi\sin\vartheta, \cos\vartheta)$, $\nu = \mu\sin(\vartheta/2)/b$, $v = \cos\phi\cos(\vartheta/2)$, $w = 1 + \nu^2/2 - \sin^2(\vartheta/2)(1-b^{-2})$, and ω is the scattered frequency as observed in the laboratory frame, which is confined by the δ functions in (1) to the discrete Doppler shifted values $\omega = l\omega_i/w$.

As is to be expected, the classical cross section (1) differs from Goldman's (1964) quantum mechanical one only by terms of the order of $\hbar\omega_i/mc^2$, which for the Nd:glass laser wavelength is approximately $2{\cdot}5\times10^{-6}$ and hence sufficiently small.

By rewriting the squared modulus in (1) as

$$|\boldsymbol{s}\times\boldsymbol{I}_l|^2 = (\cot(\vartheta/2)J_{l,0} + \mu\cos\phi\,J_{l,1}/b)^2 + (\mu\sin\phi\,J_{l,1}/b)^2, \tag{4}$$

we reduce the evaluation of the cross section (1) to the evaluation of the integrals

$$J_{l,\lambda} = \int_0^{2\pi}\cos^{\lambda}\eta\,\exp[lF(\eta)]\,\mathrm{d}\eta, \qquad \lambda = 0, 1, \tag{5}$$

which, in the notation of Brown and Kibble (1964) and Kelsey and Rosenberg (1979), can be expressed through generalised Bessel functions $C_l(\rho, \delta, \beta)$ as

$$J_{l,0} = 2\pi C_l(2lv\nu/w, l\nu^2/2w, 0) \tag{6a}$$

and

$$J_{l,1} = \pi[C_{l+1}(2lv\nu/w, l\nu^2/2w, 0) + C_{l-1}(2lv\nu/w, l\nu^2/2w, 0)]. \tag{6b}$$

Hence, by establishing in the next section a uniform asymptotic expansion of the integrals $J_{l,\lambda}$, we simultaneously provide the same for the generalised Bessel functions $C_l(\rho, \delta, \beta)$ with $\beta = 0$, this being the only case of practical importance since it corresponds to a linearly polarised laser beam, while $\beta \neq 0$ corresponds to elliptic polarisation (see e.g. Brown and Kibble 1964).

3. Uniform asymptotic expansion of scattering cross section

The standard procedure in nearly all the work where generalised Bessel functions have appeared has been to resort to circular polarisation, as in the case of Goldman (1964), for then the generalised Bessel functions reduce to ordinary ones (see e.g. Brown and Kibble 1964, Kelsey and Rosenberg 1979), although circular polarisation is of little experimental relevance since all this work has been concerned with modifications to various scattering processes under the influence of an *intense* laser field, which as remarked in the Introduction is invariably linearly polarised. Alternatively, the relation

$$C_l(\rho, \delta, 0) = \sum_{m=-\infty}^{+\infty} J_{l-2m}(-\rho) J_m(-\delta/2) \tag{7}$$

has been used (see e.g. Brown and Kibble 1964, Ehlotzky 1978, Kelsey and Rosenberg 1979), which like any straightforward series expansion of the original integral (5) is only practicable for small values of the parameters l, ρ and δ, for then it is rapidly convergent. However, one is interested in the behaviour of (6a, b) for large values of these parameters, in which case the computation of (6a) via (7) becomes excessively time consuming. Consequently, the use of (7)—although seemingly carrying the analytical development one step further—really takes one farther from obtaining actual numbers, which in the literature is borne out by the almost complete absence of graphical representations of physical quantities that have been formulated in terms of this expansion (Brown and Kibble 1964, Ehlotzky 1978, Kelsey and Rosenberg 1979).

Instead, we go back to the original integral representation (5), which as it stands cannot be used for large values of the parameters either, because of the rapid oscillations of the integrand. However, we have shown in preliminary investigations of related problems (Leubner 1978, 1979) that the integral representation (5) is well suited for standard asymptotic techniques as introduced by Chester *et al* (1957).

In the following, we will therefore use the same approach to establish in a self-contained way a uniform asymptotic expansion of (5) beyond the leading term, which a graphical comparison with the result of an exact evaluation of (5) will convincingly prove to be highly satisfactory for all present purposes. As in our previous work (Leubner 1978, 1979), the first step consists in invoking Cauchy's integral theorem to deform the original contour of integration from 0 to 2π along the real axis of the complex η-plane, where rapid oscillations occur, in such a way that no oscillations occur along the new contour, which (if we neglect the slow variations due to the presence of $\cos\eta$) is therefore characterised by $\mathrm{Im}[F(\eta)]$ being constant along it. The paths of constant $\mathrm{Im}[F(\eta)]$ through the endpoints of the original interval of integration along which $\mathrm{Re}[F(\eta)]$ decreases are easily seen to be the straight lines $\eta = \mathrm{i}y$ and $\eta = 2\pi + \mathrm{i}y$ with $0 \leqslant y < \infty$, if we set $\eta = x + \mathrm{i}y$. It remains to connect the endpoints $\mathrm{i}\infty$ and $2\pi + \mathrm{i}\infty$ of these straight lines with a path of constant $\mathrm{Im}[F(\eta)]$. To this end we first note that $\mathrm{Re}[F(\eta)] = -\infty$ *both* at $\eta = \mathrm{i}\infty$ *and* at $\eta = 2\pi + \mathrm{i}\infty$. Since, as is well known, $\mathrm{Re}[F(\eta)]$ is monotonic along an $\mathrm{Im}[F(\eta)] = \text{constant}$ path if $\mathrm{d}F/\mathrm{d}\eta$ is non-zero everywhere on it, this implies that the required path must pass through one or more saddle points of $F(\eta)$, which are characterised by $\mathrm{d}F/\mathrm{d}\eta = 0$ and hence are points where the mapping $z = F(\eta)$ is non-conformal.

As we have shown (Leubner 1978, 1979), the saddle points of $F(\eta)$ can easily be found in the case at hand, since they are determined by a quadratic equation in $\nu \cos\eta$

with solutions

$$\nu \cos \eta_S = -v \pm \mathrm{i}[w - v^2 - (\nu^2/2)]^{1/2}, \tag{8}$$

where we can restrict the analysis to $v \geqslant 0$ because (4) turns out to be invariant with respect to the substitutions $\phi \to \phi \pm \pi$. The radicand is positive semidefinite since $w - v^2 - (\nu^2/2) = \cot^2(\vartheta/2) \sin^2 \phi + \sin^2(\vartheta/2)/b^2 \geqslant 0$, so that throughout the range of allowed values of the parameters of our problem we have the same simple configuration of four saddle points, symmetrically situated in the strip $\pi/2 \leqslant x \leqslant 3\pi/2$ of the complex η-plane, as shown in figures 1(*a*) and 1(*b*) for two different sets of parameters. It therefore suffices to evaluate from (8) the coordinates of one of these saddle points, say the one denoted by S_1 in these figures, and we find

$$x_S = \cos^{-1}(-[\![\{(w + \nu^2/2) - [(w + \nu^2/2)^2 - 4v^2\nu^2]^{1/2}\}/2\nu^2]\!]^{1/2}), \tag{9a}$$

$$y_S = \cosh^{-1}([\![\{(w + \nu^2/2) + [(w + \nu^2/2)^2 - 4v^2\nu^2]^{1/2}\}/2\nu^2]\!]^{1/2}). \tag{9b}$$

The paths of constant imaginary part of $F(\eta)$ through the saddle points are determined by

$$\mathrm{Im}[F(\eta)] = \mathrm{Im}[F(\eta_S)], \tag{10}$$

and can be easily found in explicit form from (3), e.g., for the saddle point S_1, as

$$y = \cosh^{-1}\{(-v/\nu \cos x) \pm [(v/\nu \cos x)^2 - (x - \mathrm{Im}[F(\eta_S)])w/(\nu^2 \sin x \cos x) + \tfrac{1}{2}]^{1/2}\}. \tag{11}$$

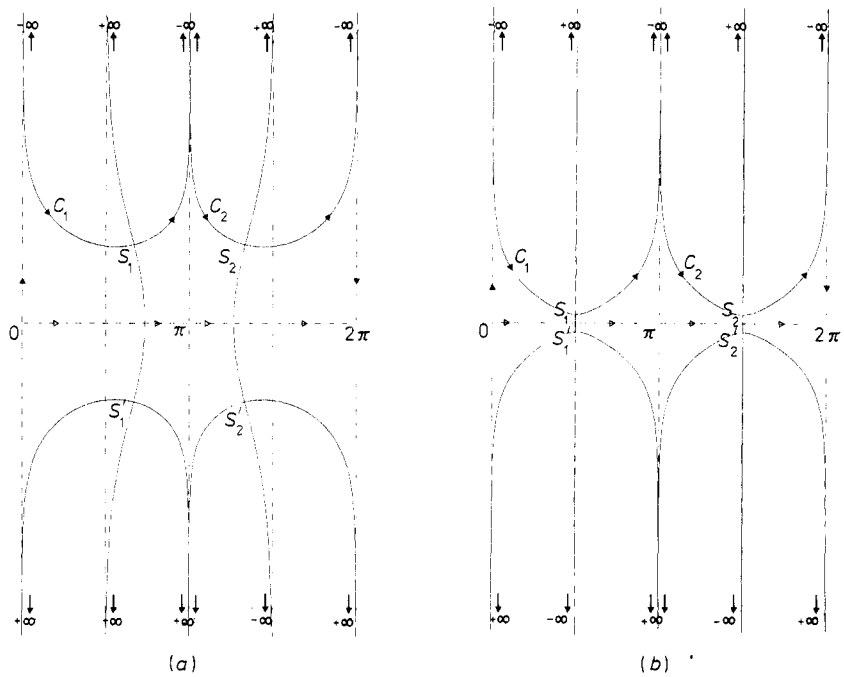

Figure 1. (*a*), (*b*) η-plane location of the four saddle points S_1, S_1', S_2, S_2' and of the paths of steepest descent and of steepest ascent of $F(\eta)$ as given by equation (3) (along which $\mathrm{Re}[F(\eta)]$ decreases to $-\infty$ and increases to $+\infty$, respectively) for two different sets of parameters $\{\mu, \vartheta, \phi, b\}$. Open arrows indicate the original path of integration, equation (5), with rapid oscillations of the integrand; solid arrows indicate the deformed contour, equation (12), along which the integrand is essentially monotonic.

Note that the two signs in front of the square root reflect the existence of two solutions to (10) in the case of a simple saddle point like S_1 (i.e. $dF/d\eta = 0$, but $d^2F/d\eta^2 \neq 0$), one being a path of steepest descent, with $\mathrm{Re}[F(\eta)]$ decreasing as we go away from S_1, the other a path of steepest ascent. In the present case, the required path of steepest descent extending from $\eta = i\infty$ through the saddle point S_1 to $\eta = \pi + i\infty$ and denoted by C_1 in figures 1(*a*) and 1(*b*) is obtained from (11) by taking the positive sign in the interval $0 < x < \pi/2$, the negative sign in the interval $\pi/2 < x \leq x_S$, and again the positive sign in the interval $x_S \leq x < \pi$. As shown in figures 1(*a*) and 1(*b*), all steepest paths through the saddle points are situated symmetrically with respect to the straight lines $y = 0$ and $x = \pi$.

So far, we have established that the original integral with a rapidly oscillating integrand can be evaluated by a contour integral over a monotonic integrand, where the contour consists of the four portions from $\eta = 0$ to $\eta = i\infty$, then along the path C_1 given by (11) through the saddle point S_1 to $\eta = \pi + i\infty$, then further along the path C_2 obtained from (11) by replacing $x \to 2\pi - x$ and $x_S \to 2\pi - x_S$, $y_S \to y_S$ to $2\pi + i\infty$, and then down to $\eta = 2\pi$, the original endpoint of integration, as shown in figures 1(*a*) and 1(*b*). By virtue of the integer value of the parameter l and of the periodicity of $F(\eta)$, we easily find that the first and fourth contributions to our contour integral cancel out, and that the third contribution is just the complex conjugate of the second one, so that

$$J_{l,\lambda} = 2\,\mathrm{Re}\Big(\exp(il\,\mathrm{Im}[F(\eta_S)]) \int_{C_1} \cos^{\lambda}\eta \exp(l\,\mathrm{Re}[F(\eta)])\,d\eta\Big), \tag{12}$$

with C_1 the steepest-descent path (11). Note that the rapidly varying portion of the integrand, which for large l caused computational problems along the original contour of integration along the real axis, is now monotonic decreasing on either side of the saddle point and the more rapidly so the larger l.

For later comparison with the uniform asymptotic expansion of (12) to be derived next, we computed the amplitude of the δ functions in the cross section (1) with the aid of (4) and the exact contour-integral representation (12) of the generalised Bessel functions. The result, exhibiting considerable fine structure, is graphically represented in figure 2(*a*).

Although the evaluation of the generalised Bessel functions (6*a*, *b*) by means of the representation (12) is for large l much more efficient than by means of the expansion (7) or by integrating from $\eta = 0$ to $\eta = 2\pi$ along the real axis, we can further reduce the computing time drastically with only a small sacrifice in accuracy by going over to an asymptotic expansion of (12).

This will be accomplished by the method of Chester *et al* (1957), where we first have to determine whether—as we vary the parameters of the problem—one or more of the saddle points S_1', S_2, S_2' approach or even coalesce with the relevant saddle point S_1. By an examination of (9*a*, *b*) we find that starting from the situation in figure 1(*b*), where S_1 is close to S_1', an appropriate variation of the parameters will induce the pairs S_1, S_1' and S_2, S_2' to approach symmetrically the point $\eta = \pi$, where the new pairs S_1, S_2 and S_1', S_2' form, which then move up and respectively down along the line $x = \pi$, so that S_1 is now close to S_2. However, only the situation depicted in figure 1(*b*) has to be taken into account, since in the situation where S_1 is close to S_2 or to all three remaining saddle points, the value of the functions (12) is negligibly small. This can be simply established by observing that the exponential in the integrand of (12) is everywhere along the contour C_1 smaller than at the saddle point. Hence, the value of $\exp(l\,\mathrm{Re}[F(\eta_S)])$ is a

measure of the value of (12), and it is found that for S_1 close to S_1' (and for large l) this quantity is many orders of magnitude larger than in the other cases.

According to the work of Chester *et al* (1957) this suggests that we obtain a uniform asymptotic expansion of (12) (i.e. uniformly valid for all parameter combinations for which the value of (12) is not negligible), if in a next step we map the η plane onto a z plane according to

$$F(\eta) = z^3/3 - d^2 z + c \equiv p_3(z), \tag{13}$$

where the third-degree mapping polynomial $p_3(z)$ exhibits the same saddle-point configuration as that relevant for $F(\eta)$ in the η plane, namely, two saddle points at $z_S = \pm d$, which are close to each other for small values of $|d|$. If we map η_{S_1} onto $z = d$ and $\eta_{S_1'}$ onto $z = -d$, we find (Leubner 1979)

$$c = \mathrm{i}\,\mathrm{Im}[F(\eta_{S_1})] \tag{14a}$$

and

$$d = (-\tfrac{3}{2}\,\mathrm{Re}[F(\eta_{S_1})])^{1/3}, \tag{14b}$$

where d is understood to be real. From (13) we have

$$\mathrm{Re}[F(\eta)] = \mathrm{Re}[p_3(z)], \qquad \mathrm{Im}[F(\eta)] = \mathrm{Im}[p_3(z)], \tag{15}$$

so that the mapping (13) transforms (12) into

$$J_{l,\lambda} = 2\,\mathrm{Re}\Big(\exp(\mathrm{i}l\,\mathrm{Im}[F(\eta_{S_1})]) \int_{C_z} \cos^\lambda \eta(z)\exp[l(z^3/3 - d^2 z)](\mathrm{d}\eta/\mathrm{d}z)\,\mathrm{d}z\Big). \tag{16}$$

The contour C_z in the z plane is given by (10) and (15) as

$$\mathrm{Im}[p_3(z)] = \mathrm{Im}[p_3(d)] = \mathrm{Im}[F(\eta_{S_1})] \tag{17a}$$

or, with (14a), as

$$\mathrm{Im}[z^3/3 - d^2 z] = 0, \tag{17b}$$

so that the integrand, apart from the slowly varying factors $\cos^\lambda \eta$ and $\mathrm{d}\eta/\mathrm{d}z$, is again monotonic decreasing on either side of the saddle point $z = d$.

So far, (16) is exact since only a transformation of variable has been performed. But Chester *et al* (1957) have shown that if this transformation of variable from the η plane to the z plane preserves the relevant configuration of saddle points, as it does in the present case, then by expanding the slowly varying factors $\cos^\lambda \eta$ and $\mathrm{d}\eta/\mathrm{d}z$ in the neighbourhood of the saddle point $z = d$ and integrating term by term, an asymptotic expansion of (16) is obtained. As we shall see presently, the inclusion of only the first few terms of this expansion will be sufficiently accurate for our purposes.

Following Chester *et al*.(1957) we now expand $\cos^\lambda \eta\ \mathrm{d}\eta/\mathrm{d}z$ in a power series of the form

$$\cos^\lambda \eta\ \mathrm{d}\eta/\mathrm{d}z = \sum_m p_m^{(\lambda)}(z^2 - d^2)^m + \sum_m q_m^{(\lambda)} z(z^2 - d^2)^m, \tag{18}$$

where the coefficients are found from repeated differentiation and use of the correspondence $\eta_S \leftrightarrow d$ and $\eta_S^* \leftrightarrow -d$. For $\lambda = 0$ we thus find

$$\begin{aligned}
p_0^{(0)} &= \mathrm{Re}(\eta_S'), \\
p_1^{(0)} &= (\mathrm{i}/2d)\,\mathrm{Im}(\eta_S''), \\
p_2^{(0)} &= (1/8d^2)\,\mathrm{Re}(\eta_S''') - (\mathrm{i}/8d^3)\,\mathrm{Im}(\eta_S''), \\
q_0^{(0)} &= (\mathrm{i}/d)\,\mathrm{Im}(\eta_S'), \\
q_1^{(0)} &= (1/2d^2)\,\mathrm{Re}(\eta_S'') - (\mathrm{i}/2d^3)\,\mathrm{Im}(\eta_S'), \\
q_2^{(0)} &= (\mathrm{i}/8d^3)\,\mathrm{Im}(\eta_S''') - (3/8d^4)\,\mathrm{Re}(\eta_S'') + (3\mathrm{i}/8d^5)\,\mathrm{Im}(\eta_S'),
\end{aligned} \tag{19}$$

where the derivatives of η with respect to z, denoted by primes, evaluated at the saddle point S_1, denoted by subscripts S, are obtained explicitly by repeated differentiation of (13) and use of (8) and of $\sin \eta_S$ which follows therefrom. By abbreviating $\cos \eta\, \eta' = \zeta'$, and differentiating this expression repeatedly, we find that the coefficients for $\lambda = 1$ are again given by (19) with η_S' replaced by ζ_S', η_S'' by ζ_S'' etc. Inserting the expansions (18) into (16) and carrying out the integrations term by term, it can easily be shown (Chester *et al* 1957) that by suitably integrating by parts the asymptotic expansion of (16) involves just the Airy function Ai and its derivative with respect to the argument Ai' in the form

$$\begin{aligned}
J_{l,\lambda} = 2\,\mathrm{Re}\Big\{ 2\pi\mathrm{i} \exp(\mathrm{i}l\,\mathrm{Im}[F(\eta_S)]) \Big[\Big(\frac{p_0^{(\lambda)}}{l^{1/3}} - \frac{q_1^{(\lambda)} + 2d^2 q_2^{(\lambda)}}{l^{4/3}} \Big) \mathrm{Ai}(l^{2/3} d^2) \\
+ \Big(-\frac{q_0^{(\lambda)}}{l^{2/3}} + \frac{2p_2^{(\lambda)}}{l^{5/3}} \Big) \mathrm{Ai}'(l^{2/3} d^2) \Big] \Big\}.
\end{aligned} \tag{20}$$

4. Discussion

In order to test the accuracy of the asymptotic expansions (20) of the $J_{l,\lambda}$'s, we computed the amplitude of the δ functions in the cross section (1) in terms of (20). The result is shown in figure 2(*b*), where the lettering is as in figure 2(*a*) but has been omitted to distinguish the two diagrams which would otherwise be almost indistinguishable. Obviously, the asymptotic expansion (20) of the generalised Bessel functions (6*a*, *b*) is capable of reproducing all the details of these functions, however, at considerably less computing time: on the relatively slow local CDC 3300 computer, the approximately 2000 points of figure 2(*a*) were generated in more than three hours, while the same number of points in figure 2(*b*) were generated in just over six minutes.

With the accurate and easily computable asymptotic expansions (20) of the generalised Bessel functions, we are now in a position to answer quantitatively and at very little calculational expense any question relating to high-intensity effects in the spontaneous incoherent backscattering of linearly polarised strong laser radiation from a relativistic electron beam. The problem depends on five relevant parameters, μ, E_{kin}, ϕ, ϑ, ω, of which only two can be varied at a time. In order to save space, we only show diagrams with $\phi = 0$, since the plane containing the direction of polarisation of the laser beam and of propagation of the electron beam is strongly favoured by the interesting high harmonic content of the emitted radiation. This is to be expected since in our classical

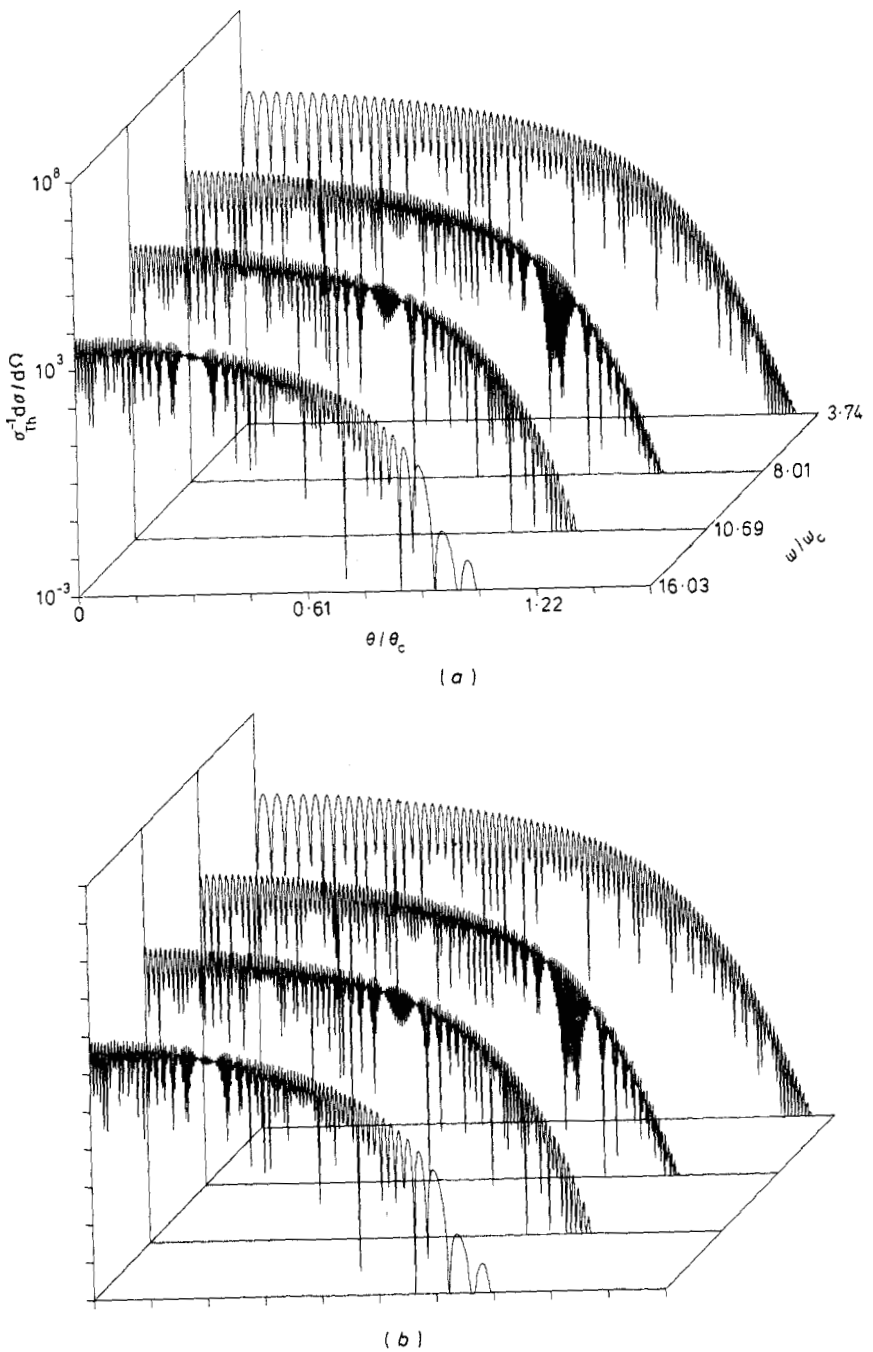

Figure 2. Comparison of the amplitude factor of the differential scattering cross section, equation (1), in units of the classical Thomson cross section σ_{Th}, as computed with the help of (*a*) the exact contour-integral representation, equation (12), of the generalised Bessel functions, and (*b*) their asymptotic expansion, equation (20), for the range of variables indicated in (*a*). The lettering in (*b*) has been omitted in order to distinguish this diagram from (*a*). Both figures were generated on the same CDC 3300 computer with (*b*) taking only $\frac{1}{30}$ of the computing time required for (*a*). $E_{kin} = 10$, $\mu = 3$, $\phi = 0$, $\theta_c = 0{\cdot}15$, $\omega_c/\omega_i = 1801$.

model, with the electrons propagating oppositely to the laser beam, the velocity of the electrons has no component perpendicular to this plane.

In order to contrast the results for linear polarisation with those for circular polarisation, we normalised the emitted frequency ω and angle of observation $\theta = \pi - \vartheta$ to the so-called critical values ω_c and θ_c of these quantities for the latter case. These are obtained by observing that in a circularly polarised electromagnetic wave of intensity μ the electron would be forced to follow a certain helical trajectory (if radiation reaction is again neglected). From the transverse acceleration corresponding to this trajectory one can then derive by Jackson's (1975) general considerations a critical frequency ω_c and a critical angle θ_c, beyond which there is very little radiation in the 'circular' case. The graphical representations for the 'linear' case, figures 2–4, show that the θ_c so derived may equally well serve as the characteristic angle for the present case, while the characteristic frequency for linear incident polarisation, especially for figures 2 and 3, is considerably larger than ω_c.

The gross features of the cross section (1), however, are of course those of a relativistic spectrum (Jackson 1975). In particular, we see that higher harmonics are confined to smaller angles θ than low ones. The same could be found from an examination of the cross section (1) for $\phi > 0$ (which we do not show), where again for fixed θ/θ_c high harmonics drop off more rapidly than low ones.

Another feature, which is also not discernible in our selection of diagrams, is that for $\mu = 1$, corresponding to an incident intensity of $I_0 = 2{\cdot}4 \times 10^{18}$ W cm^{-2}, the fundamen-

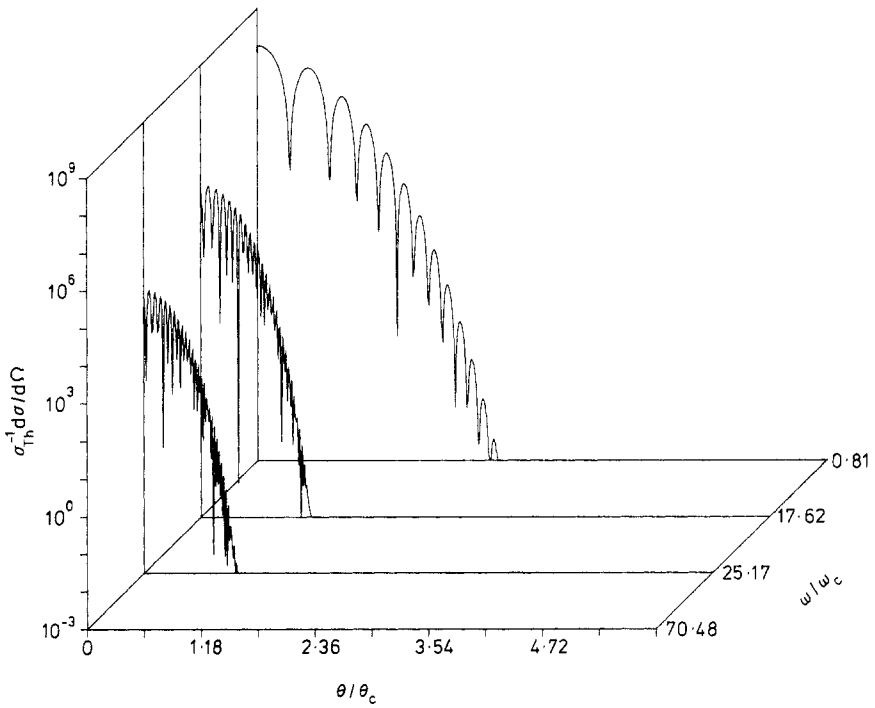

Figure 3. Plot of the amplitude factor of the differential scattering cross section, equation (1), in units of the classical Thomson cross section σ_{Th}, for sets of parameters different from figures 2(*a*) and 2(*b*). The meaning of the various symbols is as explained in the text; E_{kin} is measured in MeV, θ and θ_c in radians. $E_{kin} = 10$, $\mu = 1$, $\phi = 0$, $\theta_c = 0{\cdot}08$, $\omega_c/\omega_i = 599$.

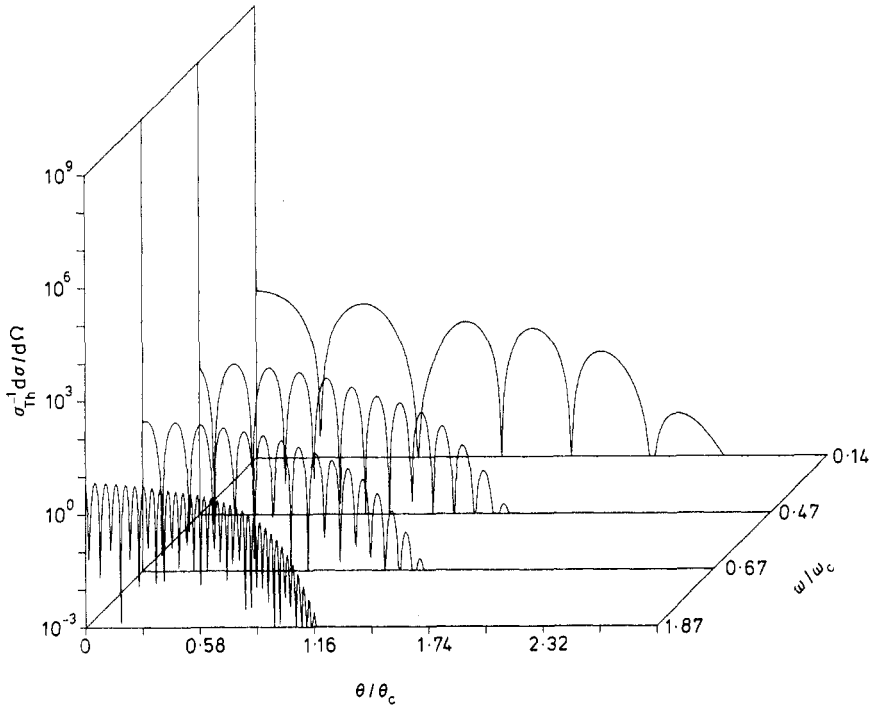

Figure 4. As figure 3, with $E_{kin} = 1$, $\mu = 3$, $\phi = 0$, $\theta_c = 1{\cdot}19$, $\omega_c/\omega_i = 43$.

tal frequency is the most intense in the scattered spectrum, while for $\mu = 3$, corresponding to $I_0 = 2{\cdot}2 \times 10^{19}$ W cm^{-2} (and more pronounced so for still higher values of μ), a whole range of scattered harmonics is more intense than the fundamental one.

Finally, by comparing figure 4 with figures 2 and 3, we note the characteristic increase in scattered power by several orders of magnitude as a result of increasing the injection energy of the electrons from $E_{kin} = 1$ MeV to $E_{kin} = 10$ MeV, a feature that was experimentally verified with incident microwave radiation by Granatstein *et al* (1976), Buzzi *et al* (1977) and Pasour *et al* (1977).

5. Conclusions

As remarked in the Introduction, even for linear incident polarisation Goldman's (1964) cross section (1) is very difficult to observe in the interesting strongly nonlinear regime because of the requirement of a coherent source of optical radiation with an intensity parameter of $\mu \gtrsim 1$. Rather, the point of general interest in the foregoing investigation is the detailed and efficient analytical treatment of the generalised Bessel function, to which Goldman's problem gives rise in a very clear-cut manner. As also elaborated upon in the Introduction, these functions occur in a number of quantum problems of current interest through the use of Volkov solutions, an important one being the study of induced bremsstrahlung in the presence of an intense laser field (see e.g. Ehlotzky 1978, Kelsey and Rosenberg 1979, Schlessinger and Wright 1979). These investigations, however, are hampered by the unavailability of efficient methods to extract actual numbers out of these functions, since unlike in Goldman's problem it

turns out (Ehlotzky 1978) that in the presence of the experimentally accessible intensity of 10^{14} W cm^{-2} one needs the behaviour of these functions for rather large values of their parameters.

Ehlotzky (1978), for example, justifiably argued that the standard description of the applied laser field in the electric dipole approximation might be inadequate in the scattering of an electron by a long-range Coulomb potential, but his analysis led to a cross section in terms of generalised Bessel functions in the unsuitable representation (7), and hence only crude qualitative estimates on the difference between the two descriptions could be given. With the help of the asymptotic representation (20), on the other hand, a quantitative evaluation of this difference would be straightforward, thus permitting a decision on the admissibility of the dipole approximation in the case of long-range potentials.

We hope that the above detailed analysis will help to reduce the number of theoretical investigations that terminate prematurely at the representation (7) of the generalised Bessel function, and that it will enable potential users to establish an asymptotic expansion analogous to (20) also under slightly modified conditions, for example, when the parameters of the problem are such that the relevant configuration of saddle points is qualitatively different from the ones shown in figures 1(a) and 1(b).

Acknowledgments

The financial support of the Österreichischer Fonds zur Förderung der wissenschaftlichen Forschung under contract 3852 is gratefully acknowledged.

References

Brehme H 1971 *Phys. Rev.* C **3** 837–40
Brown L S and Kibble T W B 1964 *Phys. Rev.* **133A** 705–18
Buzzi J M, Doucet H J, Etlicher B, Haldenwang P, Huetz A, Lamain H and Rouille C 1977 *J. Phys. Lett.* **38** L397–9
Chester C, Friedman B and Ursell F 1957 *Proc. Camb. Phil. Soc.* **53** 599–611
Denisov M M and Fedorov M V 1968 *Sov. Phys.-JETP* **26** 779–83
Ehlotzky F 1978 *Opt. Commun.* **27** 65–70
Goldman I I 1964 *Phys. Lett.* **8** 103–6
Granatstein V L, Sprangle P, Parker R K, Pasour J, Herndon M and Schlesinger S P 1976 *Phys. Rev.* A **14** 1194–201
Jackson J D 1975 *Classical Electrodynamics* 2nd edn (New York: Wiley) § 14.4
Kelsey E J and Rosenberg L 1979 *Phys. Rev.* A **19** 756–65
Landecker K 1952 *Phys. Rev.* **86** 852–5
Leubner C 1978 *Astron. Astrophys.* **69** 149–54
—— 1979 *Phys. Fluids* **22** 444–8
Lyul'ka V A 1975 *Sov. Phys.-JETP* **40** 815–8
—— 1977 *Sov. Phys.-JETP* **45** 452–6
Motz H 1951 *J. Appl. Phys.* **22** 527–35
Oleinik V P 1967 *Sov. Phys.-JETP* **25** 697–708
Pasour J A, Granatstein V L and Parker R K 1977 *Phys. Rev.* A **16** 2441–6
Schlessinger L and Wright J 1979 *Phys. Rev.* A **20** 1934–45
Stolyarov S N 1977 *Sov. J. Quantum Electron.* **7** 424–7
Tajima T and Dawson J M 1979 *Phys. Rev. Lett.* **43** 267–70
Waltz R E and Manley O P 1978 *Phys. Fluids* **21** 808–13
Yakovlev V P 1966 *Sov. Phys.-JETP* **22** 223–9